Phase Noise Resilient Codebook Design for Sparse Code Multiple Access

Haibo Liu, Qu Luo, *Member, IEEE,* Zilong Liu, *Senior Member, IEEE,*
Shan Luo, Pei Xiao, *Senior Member, IEEE*, and Xiaojun Yuan, *Senior Member, IEEE.*

***Abstract*—Sparse code multiple access (SCMA) is a promising technique for future machine type communication systems due to its superior spectral efficiency and capability for supporting massive connectivity. This paper proposes a novel class of sparse codebooks to improve the error rate performance of SCMA in the presence of phase noise (PN). Specifically, we first analyze the error rate performance of SCMA impaired by looking into the pair-wise error probability. Then, a novel codebook design metric, called minimum PN metric (MPNM), is proposed. In addition, to design PN resilient codebooks, we propose a novel pulse-amplitude modulation (PAM)-based low projection mother constellation (LP-MC), called LP-PAM. The codebooks for different users are obtained by rotating and scaling the MC, where the phase rotation angles and scaling factors for different users are optimized by maximizing the proposed MPNM. Numerical results show that the proposed PNCBs have larger MPNM values and achieve improved error rate performance than the-state-of-the-art codebooks.**

***Index Terms*—Sparse code multiple access (SCMA), phase noise, codebook design, minimum phase noise metric (MPNM).**

I. Introduction

With the widespread proliferation of Internet-of-Things (IoT) across every corner of this globe, new multiple access techniques are required to support improved spectrum efficiency and provide massive connectivity [1]. Non-orthogonal multiple access (NOMA) has emerged as a promising candidate to meet these requirements in recent years [1], [2]. Compared to the orthogonal multiple access techniques which allocate users with orthogonal time/frequency resources, NOMA allows several times more users to share the same radio resources simultaneously. This paper is concerned with sparse code multiple access (SCMA) which is a representative code-domain NOMA scheme [2]–[7].

Over the past few years, there have been a number of research attempts on SCMA codebook design [3]–[8]. By looking into the pair-wise error probability (PEP) over Gaussian and Rayleigh fading channels, it is desirable to maximize the minimum Euclidean distance (MED) and minimum product distance (MPD) of a mother constellation (MC) or a codebook. Following this design guideline, an SCMA codebook design approach based on uniquely decomposable constellation group was proposed in [5] by maximizing the MED. [8] proposed a class of power imbalanced codebook by maximizing the MED while keeping the MPD as large as possible. The SCMA codebook design has also been studied in Rician fading channels [6], [7]. Specifically, [6] and [7] have proposed a novel class codebooks for uplink and downlink Rician fading channels, respectively.

Generally speaking, the existing SCMA codebooks are mostly optimized with respect to certain wireless channel conditions but with very few considerations on the hardware impairments. The latter is particularly important for an SCMA based IoT system supporting the information exchanges over low-cost and low-end communication devices. However, existing metrics for SCMA optimization, such as MED or PEP, do not adequately capture phase noise (PN) effect, necessitating the development of a new metric tailored to this impairment. Among many others, this paper aims to develop novel sparse codebooks which are resilient to PN [9]. By looking into the PEP, we analyse the theoretical performance of SCMA system in the presence of PN and propose a new distance metric, called minimum PN metric (MPNM). We then propose a novel pulse-amplitude modulation (PAM)-based low projection mother constellation (LP-MC) for PN resilience. Finally, a novel class of PN resilient codebooks is obtained by maximizing the proposed MPNM based on the proposed LP-MC.

The rest of the paper is organized as follows: Section II introduces SCMA communication model impaired by PN. The error rate performance and the codebook design criteria of SCMA impaired by PN are introduced in Section III. Then, Section IV presents the proposed codebook by maximizing the MPNM. Numerical results are provided in Section V. Section VI concludes the paper.

II. System Model

A. SCMA Communication Model Impaired by Phase Noise

We consider a $K \times J$ SCMA system, where J users communicate over K resource nodes (RNs). The overloading factor is defined as $\lambda = J/K > 100\%$. In SCMA, each user is assigned with a unique codebook, denoted by $\boldsymbol{\mathcal{X}}_j \in \mathbb{C}^{K\times M}$, consisting of M codewords with a dimension of K. At the base station (BS) side, each SCMA encoder maps $\log_2 M$ binary bits to a length-K sparse complex codeword $\mathbf{x}_j = [x_{j,1}, x_{j,2}, \ldots, x_{j,K}]^T$ drawn from the codebook $\boldsymbol{\mathcal{X}}_j$. Each codeword has only N nonzero entries and the positions of the non-zeros elements remain the same within a codebook. Such a sparse system can efficiently represented by a factor graph which illustrates the sharing of the RNs among multiple user nodes (UNs). An SCMA factor graph with $K = 4$ and $J = 6$ is shown in Fig. 1. For a downlink SCMA system, users' data are superimposed at the BS, constituting a superimposed constellation $\boldsymbol{\Phi} \in \mathbb{C}^{K\times M^J}$ with M^J different superimposed codewords. Denote by $\mathbf{w} = \sum_{j=1}^{J} \mathbf{x}_j \in \boldsymbol{\Phi}$

Haibo Liu and Xiaojun Yuan are with the National Key Laboratory of Wireless Communications, University of Electronic Science and Technology of China (UESTC), China (e-mail: liu_hb@std.uestc.edu.cn, xjyuan@uestc.edu.cn).

Qu Luo and Pei Xiao are with 5G & 6G Innovation Centre, University of Surrey, UK (email: {q.u.luo, p.xiao}@surrey.ac.uk).

Zilong Liu is with the School of Computer Science and Electronics Engineering, University of Essex, UK (email: zilong.liu@essex.ac.uk).

Shan Luo is with the School of Aeronautics and Astronautics, UESTC, Chengdu, China (e-mail: luoshan@uestc.edu.cn).

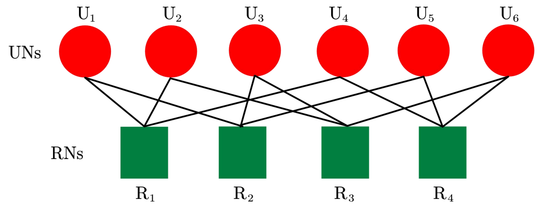

Fig. 1: An example of SCMA factor graph ($K=4,\ J=6$).

the superimposed codeword. Consider a Gaussian channel, the received signal affected by unknown PN can be expressed as [10]

$$\mathbf{r}=\mathbf{w}e^{j\boldsymbol{\theta}}+\mathbf{n}, \tag{1}$$

where $\mathbf{r}\in\mathbb{C}^{K\times 1}$ denotes the received signal vector, $\mathbf{n}=[n_1,...,n_K]^T$ denotes the complex Gaussian noise vector with its element $n_k\sim\mathcal{CN}(0,N_0)$, $\boldsymbol{\theta}=[\theta_1,\theta_2,\ldots,\theta_K]^T$ denotes the phase error vector which is subject to a Gaussian distribution with zero mean and variance σ_{p}^2, i.e., $\theta_k\sim\mathcal{N}\left(0,\sigma_{\mathrm{p}}^2\right)$. By leveraging the codebook sparsity, MPA can be employed for low-complexity decoding whose error performance approaches that of maximum likelihood (ML) receiver. Fig. 2 shows an example of the received signal at the first resource node impaired by PN, where Chen's codebook [11] and golden angle modulation (GAM) codebook [12] are considered. When PN is introduced, the constellation points in the original diagram undergo noticeable rotation, and potentially leading to overlap at higher PN levels, which increases error rates.

In the following, we will discuss the ML decision region in the presence of PN. For the communication model in (1), the likelihood based on the received signal is given by [9]

$$f(\boldsymbol{r}\mid\mathbf{w})=\prod_{k=1}^{K}\int_{-\pi}^{\pi}p(r_k\mid w_k,\theta_k)\,p(\theta_k\mid\overline{\boldsymbol{r}}_k,w_k)\,\mathrm{d}\theta_k, \tag{2}$$

where $\overline{\boldsymbol{r}}_k\triangleq[r_1,\ldots,r_{k-1},r_{k+1},\ldots,r_K]^T$ denotes the received codeword by excluding the kth symbol, and the *a posteriori* probability density function (pdf) of the PN is given by $p(\theta_k\mid\overline{\boldsymbol{r}}_k,w_k)=p(\theta_k)=\mathcal{N}\left(0,\sigma_{\mathrm{p}}^2\right)$. Then, the ML decision of the received superimposed codeword is given as

$$\hat{\mathbf{w}}\triangleq\underset{\mathbf{w}\in\boldsymbol{\Phi}}{\operatorname{argmax}}\quad f(\mathbf{r}\mid\mathbf{w}). \tag{3}$$

In the sequel, we will derive approximate expressions for the likelihood (2), which in turn allows us to obtain approximate ML detectors. These calculations play a pivotal role in the optimization process when designing new SCMA codebooks.

III. Proposed Design Criteria of Sparse Codebook in the Presence of PN

In this section, we first derive the decision rule of the received codewords with instantaneous phase error. Then, we present the proposed codebook design criteria.

A. ML Decision Rule Based on Phase Error Approximation

To derive the ML decision, we first rewrite (2) as [10]

$$\begin{aligned}f(\boldsymbol{r}\,|\,\mathbf{w})&=\prod_{k=1}^{K}\int_{-\pi}^{\pi}p(r_k\mid w_k,\theta_k)\,p(\theta_k\,|\,\overline{\boldsymbol{r}}_k,w_k)\,\mathrm{d}\theta_k\\&=\prod_{k=1}^{K}\int_{-\pi}^{\pi}p(r_k,\theta_k\,|\,w_k,\overline{\mathbf{r}}_k)\,d\theta_k=\prod_{k=1}^{K}p(r_k\,|\,w_k,\overline{\mathbf{r}}_k)\,.\end{aligned} \tag{4}$$

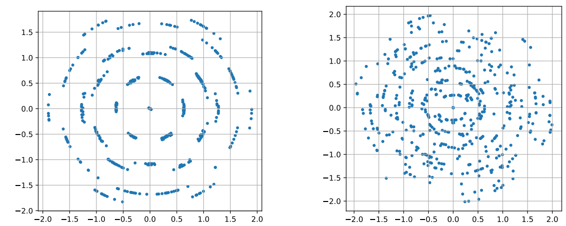

(a) Chen's codebook [11] (b) GAM [12]

Fig. 2: The effect of PN on different SCMA codebooks with $\sigma_{\mathrm{p}}^2=0.01$ and $E_b/N_0=10$dB.

Before calculating (4), we propose to approximate the received signal $\mathbf{r}$ as follows:

$$\begin{aligned}r_k&=w_ke^{j\theta_k}+n_k\\&=|w_k|\,e^{j\arg\{w_k\}}e^{j\theta_k}+n_k'e^{j\arg\{w_k\}}\\&=\left(|w_k|\,e^{j\theta_k}+n_k'\right)e^{j\arg\{w_k\}}\\&\overset{\text{(i)}}{\approx}\left(|w_k|+\Re\{n_k'\}+j\left(|w_k|\,\theta_k+\Im\{n_k'\}\right)\right)e^{j\arg\{w_k\}},\end{aligned} \tag{5}$$

where step (i) is obtained by using the approximation of $e^{j\theta_k}\approx 1+j\theta_k$, r_k denotes the kth entry of $\mathbf{r}$, and $n_k'\triangleq n_ke^{-j\arg\{w_k\}}$. In general, (i) holds tighter as σ_{p}^2 decreases. Essentially, r_k can be expressed as a 2-tuple $[\mu_k,\nu_k]$ comprising of the real and imaginary parts of r_k, where $\mu_k\triangleq\Re\left\{r_ke^{-j\arg\{w_k\}}\right\}-|w_k|\,,\nu_k\triangleq\Im\left\{r_ke^{-j\arg\{w_k\}}\right\}$. The pdf of this tuple is a bi-variate Gaussian distribution PDF conditioned on w_k, with mean value given as

$$\mathbb{E}[\mu_k,\nu_k]=\mathbb{E}\left[\Re\{n_k'\},|w_k|\,\theta_k+\Im\{n_k'\}\right]=[0\quad 0]^T, \tag{6}$$

and covariance

$$\begin{aligned}&\mathbb{E}\begin{bmatrix}|\Re\{n_k'\}|^2 & \Re\{n_k'\}\left(|w_k|\,\theta_k+\Im\{n_k'\}\right)\\ \Re\{n_k'\}\left(|w_k|\,\theta_k+\Im\{n_k'\}\right) & ||w_k|\,\theta_k+\Im\{n_k'\}|^2\end{bmatrix}\\&=\begin{bmatrix}N_0/2 & 0\\ 0 & \sigma_{\mathrm{p}}^2|w_k|^2+N_0/2\end{bmatrix}.\end{aligned} \tag{7}$$

Using (6) and (7), the conditional pdf of $\mathbf{r}$ for given $\mathbf{w}$ is

$$\begin{aligned}f(\mathbf{r}\mid\mathbf{w})&=\prod_{k=1}^{K}p(r_k\mid w_k,\bar{\mathbf{r}}_k)\\&=\frac{e^{-\frac{1}{2}\sum_{k=1}^{K}\left(\frac{\left(\Re\left\{r_ke^{-j\arg\{w_k\}}\right\}-|w_k|\right)^2}{N_0/2}+\frac{\left(\Im\left\{r_ke^{-j\arg\{w_k\}}\right\}\right)^2}{\sigma_{\mathrm{p}}^2|w_k|^2+N_0/2}\right)}}{(2\pi)^K\sqrt{(N_0/2)^K\prod_{k=1}^{K}\left(\sigma_{\mathrm{p}}^2|w_k|^2+N_0/2\right)}}.\end{aligned} \tag{8}$$

After taking negative logarithm of (8), the ML decision rule is expressed as

$$\begin{aligned}\hat{\mathbf{w}}&=\underset{\mathbf{w}\in\boldsymbol{\Phi}}{\operatorname{argmax}}\quad f(\mathbf{r}\mid\mathbf{w})\\&=\underset{\mathbf{w}\in\boldsymbol{\Phi}}{\operatorname{argmin}}\quad\left\{\sum_{k=1}^{K}\frac{\left(\Re\left\{r_ke^{-j\arg\{w_k\}}\right\}-|w_k|\right)^2}{N_0/2}\right.\\&\qquad\left.+\frac{\left(\Im\left\{r_ke^{-j\arg\{w_k\}}\right\}\right)^2}{\sigma_{\mathrm{p}}^2|w_k|^2+N_0/2}+\log\left(\sigma_{\mathrm{p}}^2|w_k|^2+N_0/2\right)\right\}\\&\triangleq\underset{\mathbf{w}\in\boldsymbol{\Phi}}{\operatorname{argmin}}\quad L_{\mathbf{w}}.\end{aligned} \tag{9}$$

B. PEP Analysis of SCMA Impaired by PN

Due to PN and Gaussian noise, the transmitted signal $\mathbf{w} \in \mathbf{\Phi}$ is assumed to be erroneously decoded to another codeword $\hat{\mathbf{w}} \in \mathbf{\Phi}, \mathbf{w} \neq \hat{\mathbf{w}}$. Denote $\Pr\{\mathbf{w} \rightarrow \hat{\mathbf{w}}\}$ by the PEP between $\mathbf{w}$ and $\hat{\mathbf{w}}$, then the average PEP, denoted as P_e, is upper-bounded by averaging over all error events, i.e.,

$$P_e \leq \frac{1}{M^J} \sum_{\mathbf{w}} \sum_{\hat{\mathbf{w}} \neq \mathbf{w}} \Pr\{\mathbf{w} \rightarrow \hat{\mathbf{w}}\}. \tag{10}$$

Moreover, by leveraging the ML decision rule derived above, we can express the probability of a pairwise error event as follows:

$$\Pr\{\mathbf{w} \rightarrow \hat{\mathbf{w}}\} = \Pr\left(L_{\mathbf{w}} - L_{\hat{\mathbf{w}}} > 0 \mid \mathbf{w}\right). \tag{11}$$

The implication of (11) is that when error decoding occurs, the performance metric $L_{\hat{\mathbf{w}}}$ becomes smaller than that of $L_{\mathbf{w}}$. For the likelihood in (9), after defining $\boldsymbol{\eta} = L_{\mathbf{w}} - L_{\hat{\mathbf{w}}}$, the difference between L_{w_k} and $L_{\hat{w}_k}$ is given as

$$\begin{aligned} \eta_k &= L_{w_k} - L_{\hat{w}_k} \\ &= \log\left(\frac{\sigma_{\mathrm{p}}^2 \left|w_k\right|^2 + N_0/2}{\sigma_{\mathrm{p}}^2 \left|\hat{w}_k\right|^2 + N_0/2}\right) \\ &\quad - \underbrace{\frac{\left(\Re\left\{re^{-j\arg\{\hat{w}_k\}}\right\} - |\hat{w}_k|\right)^2}{N_0/2}}_{\triangleq V_1} - \underbrace{\frac{\left(\Im\left\{re^{-j\arg\{\hat{w}_k\}}\right\}\right)^2}{\sigma_{\mathrm{p}}^2 \left|\hat{w}_k\right|^2 + N_0/2}}_{\triangleq V_2} \\ &\quad + \frac{\left(\Re\left\{re^{-j\arg\{w_k\}}\right\} - |w_k|\right)^2}{N_0/2} + \frac{\left(\Im\left\{re^{-j\arg\{w_k\}}\right\}\right)^2}{\sigma_{\mathrm{p}}^2 \left|w_k\right|^2 + N_0/2}. \end{aligned} \tag{12}$$

Given the superimposed codeword $\mathbf{w}$ has been transmitted, the real and imaginary parts of the received signal $\mathbf{r}$ from (5) are expressed below:

$$\begin{aligned} \Re\left\{r_k e^{-j\arg\{w_k\}}\right\} &= |w_k| + \Re\left\{n_k'\right\}, \\ \Im\left\{r_k e^{-j\arg\{w_k\}}\right\} &= |w_k|\,\theta_k + \Im\left\{n_k'\right\}, \\ \Re\left\{r_k e^{-j\arg\{\hat{w}_k\}}\right\} &= \left(|w_k| + \Re\left\{n_k'\right\}\right)\cos(\Delta_w) \\ &\quad - \left(|w_k|\,\theta_k + \Im\left\{n_k'\right\}\right)\sin(\Delta_w), \\ \Im\left\{r_k e^{-j\arg\{\hat{w}_k\}}\right\} &= \left(|w_k| + \Re\left\{n_k'\right\}\right)\sin(\Delta_w) \\ &\quad + \left(|w_k|\,\theta_k + \Im\left\{n_k'\right\}\right)\cos(\Delta_w), \end{aligned} \tag{13}$$

where $\Delta_w = \arg\{w_k\} - \arg\{\hat{w}_k\}$. Substituting (13) into (12), we obtain

$$\begin{aligned} \eta_k = &\log\left(\frac{\sigma_{\mathrm{p}}^2 \left|w_k\right|^2 + N_0/2}{\sigma_{\mathrm{p}}^2 \left|\hat{w}_k\right|^2 + N_0/2}\right) + \frac{\left(\Re\left\{n_k'\right\}\right)^2}{N_0/2} - V_1 - V_2 \\ &+ \frac{\left(\left|w_k\right|^2 \theta_k^2 + 2\left|w_k\right|\theta_k \Im\left\{n_k'\right\} + \Im^2\left\{n_k'\right\}\right)}{\sigma_{\mathrm{p}}^2 \left|w_k\right|^2 + N_0/2}, \end{aligned} \tag{14}$$

where the exact expressions of V_1 and V_2 can be found in (12). The mean values of V_1 and V_2 are respectively given by

$$E\{V_1\} = \frac{\left(|w_k|\cos\Delta_w - |\hat{w}_k|\right)^2 + |w_k|^2 \sin^2\Delta_w \sigma_{\mathrm{p}}^2 + N_0/2}{N_0/2}, \tag{15}$$

$$E\{V_2\} = \frac{|w_k|^2\left(\sin^2\Delta_w + \sigma_{\mathrm{p}}^2\cos^2\Delta_w\right) + N_0/2}{\sigma_{\mathrm{p}}^2 \left|\hat{w}_k\right|^2 + N_0/2}. \tag{16}$$

Hence, the mean value and covariance of η_k conditioned on w_k are respectively given as

$$\begin{aligned} &E_{\mathrm{PN}}\{\eta_k | w_k \rightarrow \hat{w}_k\} \\ &\quad = 2 + \log\left(\frac{\sigma_{\mathrm{p}}^2 \left|w_k\right|^2 + N_0/2}{\sigma_{\mathrm{p}}^2 \left|\hat{w}_k\right|^2 + N_0/2}\right) - E\{V_1\} - E\{V_2\} \\ &\sigma_{\mathrm{PN}}^2\{\eta_k | w_k \rightarrow \hat{w}_k\} \\ &\quad = \mathbb{E}\left\{\left(\eta_k - \mathbb{E}\left\{\eta_k \mid w_k, \hat{w}_k\right\}\right)^2 \mid w_k\right\} \\ &\quad = \mathbb{E}\left\{L_{w_k}^2 \mid w_k\right\} + \mathbb{E}\left\{L_{\hat{w}_k}^2 \mid w_k\right\} \\ &\quad\quad - 2\mathbb{E}\left\{L_{w_k} L_{\hat{w}_k} \mid w_k\right\} - \left(\mathbb{E}\left\{\eta_k \mid w_k\right\}\right)^2 \\ &\quad = 4 + 2a_k^2 + 4a_k b_k + 2c_k^2 + 4c_k d_k + 4e_k f_k \\ &\quad\quad + 4e_k g_k - 4b_k e_k - 4\sin^2(\Delta_w)(h_k + \frac{1}{i_k}) \\ &\quad\quad - 4\cos^2(\Delta_w)(1 + \frac{h_k}{i_k}), \end{aligned} \tag{17}$$

where

$$\begin{aligned} &a_k = \frac{|w_k|^2 \sin^2\Delta_w \sigma_{\mathrm{p}}^2 + N_0/2}{N_0/2}, b_k = \frac{\left(|w_k|\cos\Delta_w - |\hat{w}_k|\right)^2}{N_0/2}, \\ &c_k = \frac{|w_k|^2 \cos^2\Delta_w \sigma_{\mathrm{p}}^2 + N_0/2}{\sigma_{\mathrm{p}}^2 \left|\hat{w}_k\right|^2 + N_0/2}, d_k = \frac{|w_k|^2 \sin^2\Delta_w}{\sigma_{\mathrm{p}}^2 \left|\hat{w}_k\right|^2 + N_0/2} \\ &e_k = \frac{|w_k|^2 \sin^2\Delta_w \sigma_{\mathrm{p}}^2}{\sigma_{\mathrm{p}}^2 \left|\hat{w}_k\right|^2 + N_0/2}, f_k = \frac{|w_k|^2 \cos^2\Delta_w \sigma_{\mathrm{p}}^2}{N_0/2}, \\ &g_k = \frac{|\hat{w}_k|^2 - |w_k|^2 \cos^2\Delta_w}{N_0/2}, h_k = \frac{\sigma_{\mathrm{p}}^2 \left|w_k\right|^2 + N_0/2}{N_0/2}, \\ &i_k = \frac{\sigma_{\mathrm{p}}^2 \left|\hat{w}_k\right|^2 + N_0/2}{N_0/2}. \end{aligned} \tag{18}$$

With (17), the probability of a pairwise error event can be obtained as

$$\Pr\left(\boldsymbol{\eta} > 0 \mid \mathbf{w} \rightarrow \hat{\mathbf{w}}\right) \approx \mathcal{Q}\left(\frac{-E_{\mathrm{PN}}\{\boldsymbol{\eta} | \mathbf{w} \rightarrow \hat{\mathbf{w}}\}}{\sqrt{\sigma_{\mathrm{PN}}^2\{\boldsymbol{\eta} | \mathbf{w} \rightarrow \hat{\mathbf{w}}\}}}\right), \tag{19}$$

where $E_{\mathrm{PN}}\{\boldsymbol{\eta} | \mathbf{w} \rightarrow \hat{\mathbf{w}}\} = \sum_{k=1}^{K} E_{\mathrm{PN}}\{\eta_k | w_k \rightarrow \hat{w}_k\}$ and $\sigma_{\mathrm{PN}}^2\{\boldsymbol{\eta} | \mathbf{w} \rightarrow \hat{\mathbf{w}}\} = \sum_{k=1}^{K} \sigma_{\mathrm{PN}}^2\{\eta_k | w_k \rightarrow \hat{w}_k\}$, and $\mathcal{Q}(t) = \frac{1}{\pi}\int_0^{+\infty} \frac{e^{-\frac{x^2}{2}(t^2+1)}}{t^2+1}\mathrm{d}t$ is the Gaussian $\mathcal{Q}$-function. Substituting (19) into (10), the average PEP P_e is upper bounded by

$$P_e \leq \frac{1}{M^J} \sum_{\mathbf{w}} \sum_{\hat{\mathbf{w}} \neq \mathbf{w}} \mathcal{Q}\left(\frac{-E_{\mathrm{PN}}\{\boldsymbol{\eta} | \mathbf{w} \rightarrow \hat{\mathbf{w}}\}}{\sqrt{\sigma_{\mathrm{PN}}^2\{\boldsymbol{\eta} | \mathbf{w} \rightarrow \hat{\mathbf{w}}\}}}\right). \tag{20}$$

It should be noted that the argument of the $\mathcal{Q}$ function in (20) can be used to determine the nearest codewords in the presence of PN. To construct the optimal codebook, it is desirable to maximize the following metric:

$$\mathrm{MPNM} = \min\left\{\frac{-E_{\mathrm{PN}}\{\boldsymbol{\eta} | \mathbf{w} \rightarrow \hat{\mathbf{w}}\}}{\sqrt{\sigma_{\mathrm{PN}}^2\{\boldsymbol{\eta} | \mathbf{w} \rightarrow \hat{\mathbf{w}}\}}} \Big| \quad \forall \mathbf{w}, \hat{\mathbf{w}} \in \mathbf{\Phi}, \mathbf{w} \neq \hat{\mathbf{w}}\right\}. \tag{21}$$

which is referred to as the minimum PN metric (MPNM).

IV. Proposed PN Resilient Codebook Design

This section presents PN resilient sparse codebook design based on the proposed MPNM metric. The design steps mainly include: the generation of one-dimensional basic constellation, the construction of the N-dimension MC and the optimization of multiple sparse codebooks by maximizing MPNM.

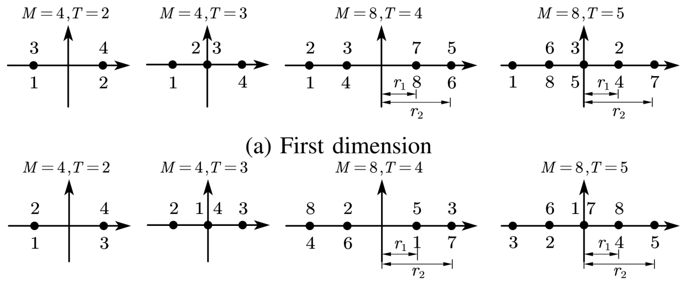

(b) Second dimension

Fig. 3: Example of $\mathcal{C}_M$ and $\pi_2^{\mathcal{T}}\left(\mathcal{C}_M\right)$.

A. LP Inspired One-dimensional Constellation Design

Based on Fig. 2, one can observe that the superimposed constellation can be well distinguished from the PN if it has less unique constellation points. This can be achieved by allowing certain overlapping within the same dimension. Due to the multidimensional nature, two transmitted codewords with overlapped constellation elements can be distinctly separated in other dimensions. Such codebook is called LP codebook in [7], and the proposed MC is called LP-MC. Motivated by this feature, a new PAM-based MC, called LP-PAM, is proposed for suppressing PN. The length-M one-dimensional LP-PAM constellation, denoted by $\mathcal{C}_M$, is composed of T distinct elements and $M-T$ overlapped points. Specifically, the construction of length T vector $\mathcal{C}_T$ is summarized as followed: for even T, generate T PAM points; for odd T, generate $T-1$ PAM points and add the original point to $\mathcal{C}_T$. For example, for even T, the one-dimensional PAM constellation $\mathcal{C}_T$ can be expressed as

$$\begin{aligned}\mathcal{C}_T &= \left[z_{1,1}, z_{1,2}, \ldots, z_{1,T}\right] \\ &= \left[-r_{T/2}, -r_{T/2-1}, \ldots, -r_1, r_1, \ldots, r_{T/2}\right],\end{aligned} \tag{22}$$

and $\alpha_m = r_{m+1}/r_1 \in (1, +\infty), \quad m = 1, 2, \ldots, T/2-1$. Then, to obtain $\mathcal{C}_M$, $M-T$ points in $\mathcal{C}_T$ must be overlapped, where the following two rules are applied to guide the selection of overlapped constellations: 1) The constellation points with lower energy are preferentially overlapped to construct $\mathcal{C}_M$, such that $\mathcal{C}_{\text{MC}}$ has a small average energy; 2) The overlapped constellation points should also exhibit certain symmetry, such that $\mathcal{C}_M$ is also symmetrical and with a zero mean.

B. Construction of the N-dimension MC

After obtaining the one-dimensional constellation $\mathcal{C}_M$, the remaining $N-1$ dimensions may be obtained by the permutation of $\mathcal{C}_M$. Let π_n denote the permutation mapping of the nth dimension. Then the N-dimensional $\mathcal{C}_{\text{MC}} \in \mathbb{C}^{N\times M}$ can be obtained as

$$\mathcal{C}_{\text{MC}} = \left[\pi_1^{\mathcal{T}}\left(\mathcal{C}_M\right), \pi_2^{\mathcal{T}}\left(\mathcal{C}_M\right), \ldots, \pi_N^{\mathcal{T}}\left(\mathcal{C}_M\right)\right]^{\mathcal{T}}. \tag{23}$$

The goal is to find the N permutations $\pi_n, n = 1, 2, \cdots, N$ for maximizing the minimum Euclidean distance of $\mathcal{C}_{\text{MC}}$. In this paper, the minimum Euclidean distance (MED) is considered as permutation metric and the the binary switching algorithm is employed to find the N permutations [7]. Next, we give an example of the proposed $\mathcal{C}_M$ and $\pi_2^{\mathcal{T}}\left(\mathcal{C}_M\right)$ in Fig. 3, where $\alpha_1 = r_2/r_1$ is a parameter to be optimized.

C. Optimization of Sparse Codebooks

Upon obtaining $\mathcal{C}_{\text{MC}}$, phase rotations and energy scaling are applied to generate multiple sparse codebooks in order to enhance the distance properties of the superimposed codewords [7]. Specifically, user j's sparse codebook is designed as $\mathcal{C}_j = \mathbf{E}_j\mathbf{R}_j\mathcal{C}_{\text{MC}}$, where $\mathbf{R}_j$ and $\mathbf{E}_j$ denote the phase rotation matrix and power scaling matrix of user j, respectively. For simplicity, we define a constellation operator matrix as $\mathbf{\Psi}_j = \mathbf{E}_j\mathbf{R}_j$. For a $\mathcal{C}_{\text{MC}}$ with $N=2$, $\mathbf{E}_j$ and $\mathbf{R}_j$ can be expressed as

$$\mathbf{E}_j = \begin{bmatrix} E_1 & 0 \\ 0 & E_2 \end{bmatrix}, \mathbf{R}_j = \begin{bmatrix} e^{j\theta_1} & 0 \\ 0 & e^{j\theta_2} \end{bmatrix}, \mathbf{\Psi}_j = \begin{bmatrix} \psi_1 & 0 \\ 0 & \psi_2 \end{bmatrix} \tag{24}$$

where $\psi_i = E_i e^{j\theta_i}, \forall E_i > 0, 1 \le i \le N$. Then, user j's codebook can be generated by $\boldsymbol{\mathcal{X}}_j = \mathbf{V}_j\mathbf{\Psi}_j\mathcal{C}_{\text{MC}}$, where $\mathbf{V}_j$ is the binary mapping matrix that maps an N-dimensional dense constellation to a K-dimensional sparse codebook. We further combine the constellation operation matrix $\mathbf{\Psi}_j$ and mapping matrix $\mathbf{V}_j$ together, i.e., $\boldsymbol{\mathcal{V}}_j = \mathbf{V}_j\mathbf{\Psi}_j$. In this paper, for the SCMA system given in Fig. 1, the mapping matrices are designed as

$$\begin{aligned}&\boldsymbol{\mathcal{V}}_1 = \begin{bmatrix} \psi_1 & 0 \\ 0 & 0 \\ 0 & \psi_3 \\ 0 & 0 \end{bmatrix}, \boldsymbol{\mathcal{V}}_2 = \begin{bmatrix} 0 & 0 \\ \psi_1 & 0 \\ 0 & 0 \\ 0 & \psi_3 \end{bmatrix}, \boldsymbol{\mathcal{V}}_3 = \begin{bmatrix} \psi_2 & 0 \\ 0 & \psi_2 \\ 0 & 0 \\ 0 & 0 \end{bmatrix}, \\ &\boldsymbol{\mathcal{V}}_4 = \begin{bmatrix} 0 & 0 \\ 0 & 0 \\ \psi_2 & 0 \\ 0 & \psi_2 \end{bmatrix}, \boldsymbol{\mathcal{V}}_5 = \begin{bmatrix} \psi_3 & 0 \\ 0 & 0 \\ 0 & 0 \\ 0 & \psi_1 \end{bmatrix}, \boldsymbol{\mathcal{V}}_6 = \begin{bmatrix} 0 & 0 \\ \psi_3 & 0 \\ 0 & \psi_1 \\ 0 & 0 \end{bmatrix}.\end{aligned} \tag{25}$$

Hence, based on the proposed multi-dimensional codebook construction scheme, the design of sparse codebook can be formulated as

$$\begin{aligned}\mathcal{P}: \max_{\mathbf{E},\boldsymbol{\theta},\boldsymbol{\alpha}} \quad & \text{MPNM}(\mathcal{X}) \\ \text{Subject to} \quad & \sum_{i=1}^{d_f} E_i = \frac{MJ}{K}, E_i > 0, \\ & 0 \le \theta_i \le \pi, \forall i = 1, 2, \ldots, d_f, \\ & \alpha_m \ge 1, m = 1, 2, \ldots, T/2-1.\end{aligned} \tag{26}$$

where rotation angles $\boldsymbol{\theta} = \left[\theta_1, \theta_2, \ldots, \theta_{d_f}\right]^{\text{T}}$, energy factors $\mathbf{E} = \left[E_1, E_2, \ldots, E_{d_f}\right]^{\text{T}}$ and scattering factors $\boldsymbol{\alpha} = \left[\alpha_1, \alpha_2, \ldots, \alpha_{T/2-1}\right]^{\text{T}}$ are the parameters to be optimized. Unfortunately, the optimization in (26) is difficult to solve due to the non-convex objective function. Similar to existing constellation and SCMA codebook design works [7], [9], [13], we solve (26) with a numerical global search method by using the MATLAB Global Optimization Toolbox.

V. Numerical Results

This section conducts numerical evaluations for the proposed PNCBs. In addition to the SCMA system with $K=4, J=6$, we also consider an SCMA system with larger size, i.e., $K=5, J=10$, where the mapping matrices in [7] is employed. Given that the proposed criteria are designed for high E_b/N_0 regimes, we choose $E_b/N_0 = 14$ dB for optimization. The PNCBs designed with $T=2$ and 3 for $M=4, \lambda=150\%$ are named as PNCB_1 and PNCB_2, respectively. The designed PNCBs with $T=4$ and 5 for $M=8, \lambda=150\%$ are named as PNCB_3 and PNCB_4, respectively, and the PNCBs with $T=2$ and 3 for $M=4, \lambda=200\%$ are named as PNCB_5 and PNCB_6, respectively. For comparison, we consider Chen's codebook [11], GAM codebook [12] and StarQAM codebook [13]. Specifically,

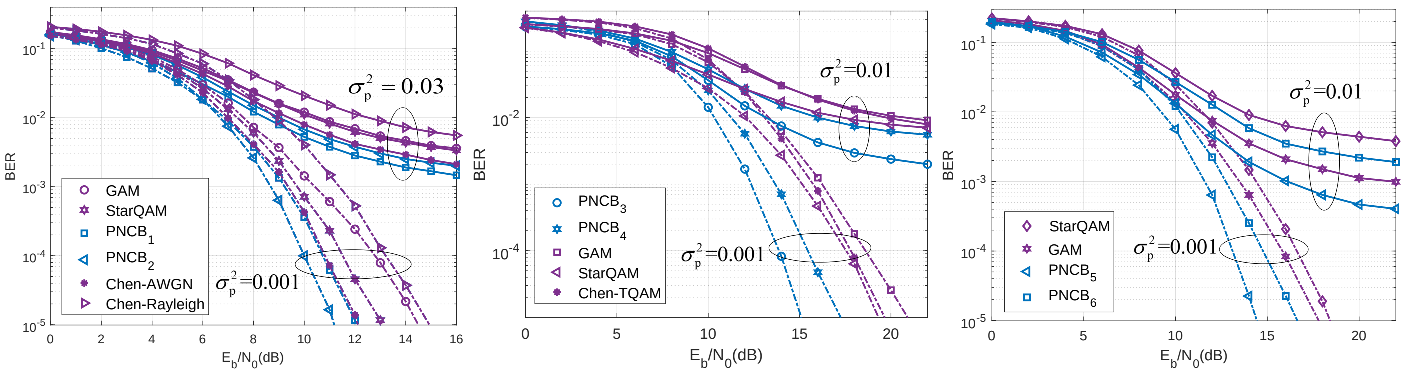

(a) $M = 4, \lambda = 150\%$.

(b) $M = 8, \lambda = 150\%$.

(c) $M = 4, \lambda = 200\%$.

Fig. 4: BER performance comparison of different codebooks under different PN levels.

TABLE I: MPNM and MED values of different codebooks.

System setting	σ_p^2	Codebook	MPNM	MED
$M = 4, \lambda = 150\%$ $E_b/N_0 = 10$ dB	0.03	StarQAM	1.45	0.9
		GAM	1.31	0.57
		Chen-AWGN	1.68	1.1
		Chen-Rayleigh	1.25	0.65
		PNCB$_1$	1.85	1.06
		PNCB$_2$	1.70	1.19
$M = 8, \lambda = 150\%$ $E_b/N_0 = 15$ dB	0.01	StarQAM	3.40	0.45
		GAM	2.82	0.47
		Chen-TQAM	3.32	0.49
		PNCB$_3$	3.95	0.64
		PNCB$_4$	3.82	0.51
$M = 4, \lambda = 200\%$ $E_b/N_0 = 15$ dB	0.01	StarQAM	2.65	0.48
		GAM	4.4	0.43
		PNCB$_5$	5.1	0.88
		PNCB$_6$	3.38	0.59

the codebooks designed in [11] for AWGN and Rayleigh fading channels with $M = 4$ are referred to as Chen-AWGN and Chen-Rayleigh codebooks, respectively, and the TQAM codebook with $M = 8$ is also considered.

Table I compares the MPNM and MED values of the proposed PNCBs with Chen [11], GAM [12] and StarQAM [13] codebooks for different systems. It is shown that the MPNMs of the proposed codebooks are larger than that of the other codebooks. It should be noted that the codebook with a larger MPNM value enjoy improved BER performance, and the MPNM values in Table I are consistent with the BER performance shown in Fig. 4.

Fig. 4a compares the BER performance of different codebooks for $M = 4, \lambda = 150\%$ under different PN levels. For $\sigma_p^2 = 0.001$, the proposed PNCB_1 and PNCB_2 respectively achieve about 0.7 and 1.5 dB gains over StarQAM at $\mathrm{BER} = 10^{-4}$ and PNCB_1 performs slightly better than Chen-AWGN. However, for a large PN with $\sigma_p^2 = 0.03$, the proposed PNCB_2 achieves the best BER performance among all codebooks. Fig. 4b and Fig. 4c compare the BER performance of different codebooks for $M = 8, \lambda = 150\%$ and $M = 4, \lambda = 200\%$ under different PN levels, respectively. As can be seen from Fig. 4b, the proposed PNCB_3 and PNCB_4 achieve better performance than other codebooks for both $\sigma_p^2 = 0.01$ and $\sigma_p^2 = 0.001$. In Fig. 4c, the gain of the proposed PNCB_5 is more prominent, with about 2 and 5 dB gains over GAM at the $\mathrm{BER} = 10^{-3}$ for $\sigma_p^2 = 0.001$ and $\sigma_p^2 = 0.01$, respectively.

VI. Conclusion

This paper is devoted to PN resilient SCMA codebook design in downlink channels. First, a novel distance metric named as MPNM has been devised by investigating the PEP of SCMA impaired by PN. Then, an LP-PAM-based MC has been proposed, followed by the sparse codebook construction based on the LP-PAM. In addition, the proposed PNCBs are obtained by maximizing the proposed MPNM. Finally, numerical results have been conducted to demonstrate the superior error performance under PN impairments for both $K = 4, J = 6$ and $K = 5, J = 10$ SCMA systems.

References

[1] Z. Liu and L.-L. Yang, "Sparse or dense: A comparative study of code-domain NOMA systems," *IEEE Trans. Wireless Commun.*, vol. 20, no. 8, pp. 4768–4780, 2021.

[2] Q. Luo, Z. Liu, G. Chen, and P. Xiao, "Enhancing signal space diversity for SCMA over Rayleigh fading channels," *IEEE Trans.on Wireless Commun.*, pp. 1–1, 2023.

[3] Y.-M. Chen, P.-H. Wang, C.-S. Cheng, and Y.-L. Ueng, "A joint design of SCMA codebook and PTS-based PAPR reduction for downlink OFDM scheme," *IEEE Trans. Veh. Techno.*, vol. 71, no. 11, 2022.

[4] M. Taherzadeh, H. Nikopour, A. Bayesteh, and H. Baligh, "SCMA codebook design," in *2014 IEEE VTC2014-Fall*, 2014, pp. 1–5.

[5] X. Zhang, D. Zhang, L. Yang, G. Han, H.-H. Chen, and D. Zhang, "SCMA codebook design based on uniquely decomposable constellation groups," *IEEE Trans. Wireless Commun.*, vol. 20, no. 8, pp. 4828–4842, 2021.

[6] T. Lei, S. Ni, N. Cheng, S. Chen, and X. Song, "SCMA codebook for uplink Rician fading channels," *IEEE Commun. Lett.*, vol. 27, no. 2, pp. 527–531, 2023.

[7] Q. Luo *et al.*, "A design of low-projection SCMA codebooks for ultra-low decoding complexity in downlink IoT networks," *IEEE Trans. Wireless Commun.*, vol. 22, no. 10, pp. 6608–6623, 2023.

[8] X. Li, Z. Gao, Y. Gui, Z. Liu, P. Xiao, and L. Yu, "Design of power-imbalanced SCMA codebook," *IEEE Trans. Vehi. Techno.*, vol. 71, no. 2, pp. 2140–2145, 2022.

[9] P. Y. Kam, S. S. Ng, and T. S. Ng, "Optimum symbol-by-symbol detection of uncoded digital data over the Gaussian channel with unknown carrier phase," *IEEE Trans. Commun.*, vol. 42, no. 8, pp. 2543–2552, 1994.

[10] R. Krishnan, M. R. Khanzadi, T. Eriksson, and T. Svensson, "Soft metrics and their performance analysis for optimal data detection in the presence of strong oscillator phase noise," *IEEE Trans. Commun.*, vol. 61, no. 6, pp. 2385–2395, 2013.

[11] Y.-M. Chen and J.-W. Chen, "On the design of near-optimal sparse code multiple access codebooks," *IEEE Transactions on Communications*, vol. 68, no. 5, pp. 2950–2962, 2020.

[12] Z. Mheich, L. Wen, P. Xiao, and A. Maaref, "Design of SCMA codebooks based on golden angle modulation," *IEEE Trans. Veh. Techno.*, vol. 68, no. 2, pp. 1501–1509, 2019.

[13] L. Yu, P. Fan, D. Cai, and Z. Ma, "Design and analysis of SCMA codebook based on Star-QAM signaling constellations," *IEEE Trans. Veh.Techno.*, vol. 67, no. 11, pp. 10 543–10 553, 2018.